THE INFLUENCE OF IMPINGING BOUNDARY LAYER VORTICITY PACKETS ON TURBULENT JUNCTURE FLOW BEHAVIOR

Bonnie Marini
Siemens Westinghouse Power Corporation
4400 Alafaya Trail, MC 267, Orlando FL 32836-2399, USA
bonnie.marini@swpc.siemens.com

Charles R. Smith
Department of Mechanical Engineering and Mechanics, Lehigh University
Bethlehem, Pa 18015, USA
crs1@lehigh.edu

ABSTRACT
An experimental study of the impact of a tip clearance gap in a turbulent juncture flow provides quantitative data, which suggests that the transport and amalgamation of vorticity packets in the impinging boundary layer strongly influence both the development and unsteady behavior of turbulent juncture flows. It is this sporadic, but continued, interaction with boundary layer vortex packets that sustains the strength of the turbulent horseshoe vortex system, and precipitates the unsteady behavior of the system. The presence of a clearance gap beneath the bluff body juncture allows these impinging vorticity packets to escape the juncture region, which results in a less stable, weaker horseshoe vortex system, particularly as the clearance gap is increased.

BACKGROUND
A turbulent approach juncture flow is the result of the presence of the strong adverse pressure gradient generated as the impinging flow decelerates on approach to the leading edge of a bluff body. This adverse gradient causes a strong deceleration and local flow reversal of the impinging endwall boundary layer, resulting in the formation of a turbulent horseshoe vortex system, schematically represented in figure 1. The prominent features of this horseshoe vortex system are: (1) a dominant horseshoe vortex, which results from the organization of boundary layer vorticity upstream of the juncture; (2) a secondary vortex, which is generated by the viscous interaction between the horseshoe vortex and the near-wall fluid; and (3) a tertiary vortex. In the near corner of the juncture, a small, stable, resident corner vortex also forms, rotating counter to the horseshoe vortex. Although the horseshoe vortex is a permanent flow structure of a juncture flow, the vortex system exhibits a quasi-cyclic, aperiodic unsteadiness (Praisner 1998, Sabatino 2000). During this process, the secondary vortex cyclically gains strength through viscous interaction with the horseshoe vortex, and subsequently ejects into the freestream (figure 1b) as a concentrated region of positive vorticity (opposite in sign from the horseshoe vortex). This ejection of vorticity correlates with a reduction in the vortical strength of the horseshoe vortex. The weakened horseshoe vortex subsequently entrains additional negative vorticity from the surrounding flow, is re-energized, and the process repeats.

The objective of the present study is to examine the effect of the vortical flow structure of the impinging turbulent boundary layer on the quasi-cyclic behavior of this horseshoe vortex system.

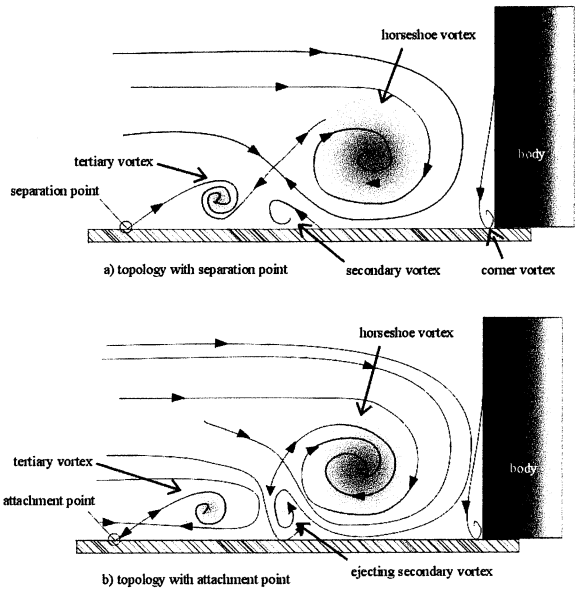

Figure 1 : Turbulent juncture flow topology

EXPERIMENTAL METHOD
To study the vortical interactions, digital particle imaging velocimetry (DPIV) was used. The result is temporal sequences of instantaneous, quantitative

velocity fields that can be digitally transformed to a sequence of vorticity fields and viewed over time.

Experiments were performed using a closed-circuit, free-surface, 6000 liter water channel with a test plate elevated 10.2 cm above the channel floor. The channel test section is 5.0 m long x 0.9 m wide x 0.4-m deep of 1.9-cm thick polycarbonate, with a speed range of 0.01 m/s to 0.4 m/s, ±2% spanwise uniformity, and a turbulence intensity of ± 0.2%. (See Acalar and Smith, 1987 for channel details). The turbulent boundary layer was established on a 3.35 meter long, 1.2 cm thick, Plexiglas flat plate with a 5:1 elliptical leading edge. The coordinate system for this study is shown in figure 2.

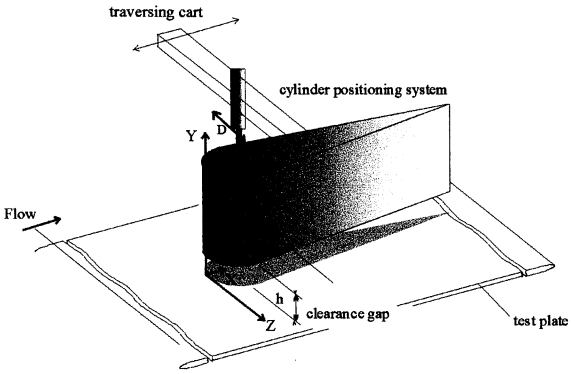

Figure 2 : Experimental arrangement and coordinate system

The boundary layer was 'tripped' using a threaded rod located approximately 2 cm from the leading edge of the plate. The freestream velocity was held at 20 cm/sec, yielding a Re_D of 3.0×10^4 and a Re_L of 5.1×10^5 (where L is the distance from the trip wire to the juncture). The flow conditions are summarized in table 1.

Table 1: Impinging boundary layer characteristics

U_o (cm/s)	20
L (cm)	253
ν (m^2/s^2)	1.00E-02
Re_x	5.1E+05
Re_D	3.0E+04
δ^*(mm)	4.5
θ (mm)	3.4
u_τ(m/s)	5.31×10^{-3}

To modify the juncture region, a clearance gap was introduced between the body and the end wall surface. Gap clearances were set using a calibrated scale inserted directly into the flow, and could be established within a maximum uncertainty of +/- 0.52 mm.

A 15.2 cm diameter tapered cylinder with a 4.6:1 taper is used as the flow obstruction. The cylinder vertical traverse mount incorporates a lockable worm gear mounted from above, which allows adjustment of the gap between the cylinder and the plate. For the present study, the symmetry plane of the body was kept parallel to the flow direction. The cylinder and traverse are mounted on a traversing cart above the test plate, as shown in figure 2.

The DPIV system, shown in figure 3, employs a modification of a high image density film-based technique (Rockwell et.al. 1993, Adrian 1991), and uses a scanning laser sheet to illuminate a suspension of neutrally-buoyant, spherical silver-coated particles with a mean diameter of 12μm and a density of 1.4 g/cc. The channel is seeded with particles to a concentration of approximately 0.003 grams per liter of water. The laser sheet is generated using a rotating, 72-facet mirror with a variable-frequency speed control, an optical focusing assembly, and a LEXEL 10 watt argon-ion laser. The laser sheet is positioned to illuminate the symmetry plane immediately upstream of the cylinder. A rotating bias mirror is oriented at a 45-degree angle immediately in front of a Pulnix TM-9701 progressive scan, black-and-white CCD video camera lens, and applies a uniform bias velocity to all images, allowing correction of directional ambiguities in flow reversal regions. The rotating mirror frequency and triggering of the bias mirror are synchronized with the video camera output signal. Synchronization is accomplished using a DPIV controller designed in house. Digital images are processed using a single-frame autocorrelation over an interrogation window of 32 x 32 pixels, with a 50% overlap.

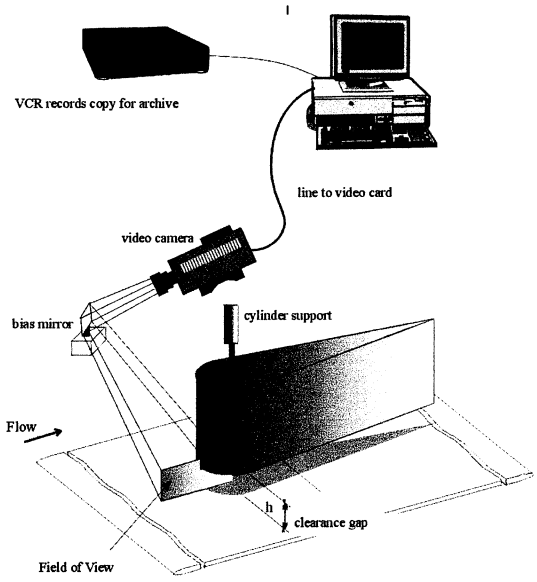

Figure 3 : Digital PIV system

The uncertainty of the velocities determined using the DPIV method is estimated at ±5%, and the maximum uncertainty of the vorticity magnitudes calculated from these velocities is ±6% (Marini, 2000).

RESULTS AND DISCUSSION

When no clearance gap is present, the quasi-cyclic behavior of the horseshoe vortex system consists of basically two stages: a) secondary vortex ejection, and b) secondary vortex reformation. The strength of the primary horseshoe vortex fluctuates during this cycle, but the vortex remains coherent. When a clearance gap is introduced, a four-stage cycle of behavior can be identified for the horseshoe vortex system: a) vorticity organization; b) the development of a quasi-steady horseshoe; c) vortex weakening; d) vortex ingestion into the clearance gap. When a small gap is present, the modifications of the cycle, compared to the no gap case, are minimal. The vortex ingestion stage occurs, but only sporadically, and the subsequent vortex reorganization is swift. As the gap clearance is increased, the temporal duration of each stage is modified. Generally, the process of vorticity organization occurs more slowly, the developed quasi-steady horseshoe vortex is present for a shorter period and weakens more rapidly, and horseshoe vortex ingestion into the clearance gap becomes a more consistent, cyclic event.

Detailed observation and assessment of the sequential DPIV fields indicates that manifold vortical interactions of the horseshoe vortex system with impinging boundary layer vorticity act to regulate the behavior and strength of the horseshoe vortex. The horseshoe vortex is supplied and maintained with vorticity from the upstream endwall boundary layer, with a portion of this impinging vorticity input due to amalgamation of the horseshoe vortex with vorticity packets, which are carried downstream from turbulent bursting events occurring well upstream of the juncture region (Sabatino 2000). This process of continued vorticity amalgamation results in the strengthening of the horseshoe vortex. However, the viscous interaction of the horseshoe vortex with endwall surface fluid stimulates the cyclic formation of secondary vortices, which consequently act to dissipate the horseshoe vortex vorticity. As a secondary vortex gains strength, it enlarges and acts as a barrier between the impinging boundary layer (the vorticity supply), and the horseshoe vortex. When this secondary vortex is ejected into the outer flow, the horseshoe vortex is re-exposed to and re-energized by the upstream boundary layer vorticity, and the growth-decay cycle of the horseshoe vortex repeats.

The horseshoe vortex for a juncture flow with no clearance gap maintains a vorticity balance. However, when a gap is introduced, this balance is upset, with weakening effects outpacing strengthening influences. Thus, the horseshoe vortex, through both viscous dissipation and advection into the clearance gap, periodically weakens and can disappear from the juncture region.

Examination of a sequence of instantaneous vorticity field plots suggests that the amalgamation of advected packets of negative vorticity with the horseshoe vortex is a primary mechanism by which the horseshoe vortex gains strength. These packets are discrete vortical products of upstream bursting that appear to remain coherent as they advect with the flow field. Figure 4 is a sequence of images for the no gap case, which illustrate this process of temporal transport of packets of negative vorticity.

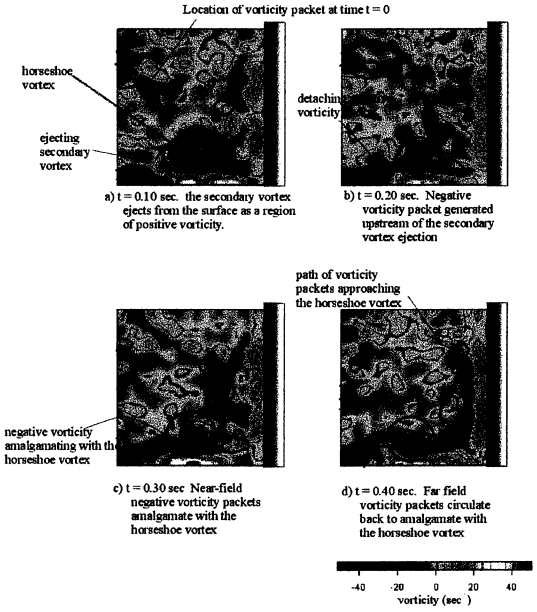

Figure 4 : Vorticity contours for no clearance gap

There appear to be two distinct types of negative vorticity packets; 1) packets of negative vorticity that advect toward the bluff body, but are well away from the end-wall surface, and 2) packets that eject from the boundary layer immediately upstream of the horseshoe vortex. These shall be referred to respectively as far-field vorticity packets and near-field vorticity packets.

Far-field vorticity packets are believed to be associated with hairpin vortices in the impinging turbulent boundary layer, and are products of upstream boundary layer bursting (Adrian et. al. 1999, Sabatino 2000). In contrast, near-field vorticity packets appear to be byproducts of the interaction of the secondary vortex with the approaching boundary layer. Upstream of the horseshoe vortex, a secondary vortex forms due to

viscous effects. This secondary vortex periodically ejects into the freestream, carrying positive vorticity with it. Concurrently, an ejection of negative vorticity is observed to develop immediately upstream of the secondary vortex ejection. It appears that the viscous interaction between the boundary layer and the bursting secondary vortex causes adjacent boundary layer fluid of negative vorticity to be dragged up and to break free of the boundary layer. This packet of released vortical fluid does not follow the secondary vortex burst throughout its ejection path, but appears to become entrained in the boundary layer just above the endwall surface, and remains relatively close to the endwall as the near-field vorticity packet advects downstream (as shown schematically in figure 5) Figure 4 shows instantaneous vorticity patterns for a recorded sequence in which such an ejection of near-wall negative vorticity boundary layer fluid occurs. Figure 6 shows the same image with the superimposed instantaneous streamlines.

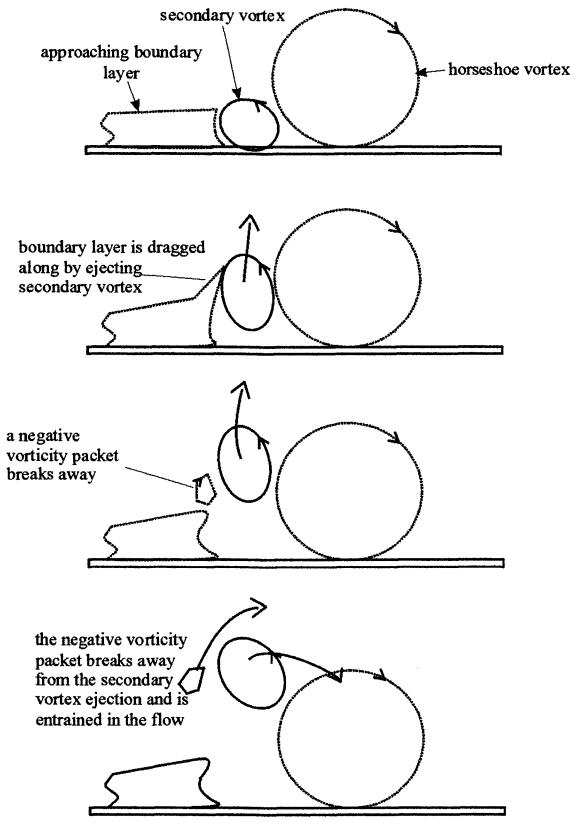

Figure 5 : Near field negative vorticity packet formation

As the far-field vorticity packets advect downstream and approach the body, they divert toward the endwall (figures 4 and 6). For the no gap case, as the vorticity packets approach the endwall they move downward and back upstream, where they amalgamate with the horseshoe vortex. Thus, boundary layer vorticity ejected from upstream "bursts" is fed back into the horseshoe vortex, which maintains the vortex strength, and compensates for the weakening effects of viscous dissipation. This process apparently helps keep the horseshoe vortex relatively stable.

Near-field vorticity packets that eject immediately upstream of the horseshoe vortex appear to move under the secondary vortex, with its associated positive vorticity, and are entrained in the flow immediately above the horseshoe vortex. These near-field vorticity packets approach the horseshoe vortex system from both upstream and above. The close proximity of the packets to the horseshoe vortex enables efficient amalgamation, with a large percentage of these near-field vorticity packets appearing to amalgamate with the horseshoe vortex.

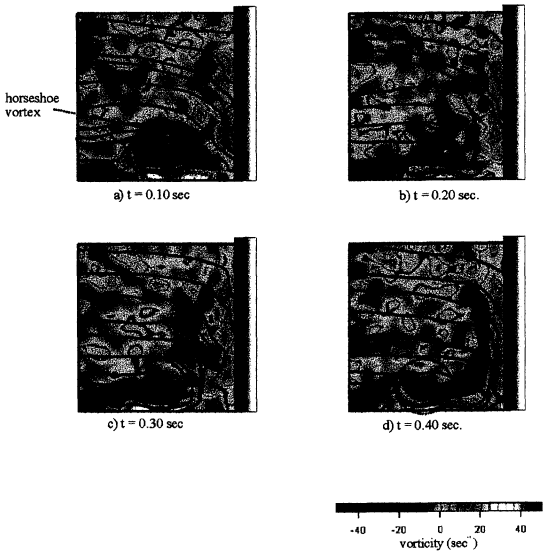

Figure 6 : Streamlines overlaid on figure 4

When a small clearance gap (1.7%D) is introduced beneath the bluff body, the near-field vorticity packets, which are in close proximity to the horseshoe vortex, still appear to be generated and amalgamate with the horseshoe vortex. However, a portion of the far-field vorticity packets does not amalgamate with the horseshoe vortex, but bypass the vortex and move directly into the clearance gap. In the freestream, the far-field vorticity packets again divert toward the endwall as they approach the body. However, presence of a clearance gap provides a new path for vorticity advection, and many of the far-field vorticity packets move down toward the endwall and into the clearance gap. Thus, these ingested packets of negative vorticity will not amalgamate with and reinforce the vorticity of the horseshoe vortex. The remaining sources of negative vorticity are not sufficient to maintain the

horseshoe vortex strength, and the weakened horseshoe vortex will subsequently move toward the body. If it is weakened sufficiently, and closely approaches the body, it can be entrained by the strong downflow layer and be swept into the clearance gap. Subsequent reorganization of the impinging vorticity field will cause the horseshoe vortex to either strengthen, or reform (if it has been ingested into the clearance gap).

If the clearance gap is increased to 3%D (figure 7), the near-field vorticity packets continue to amalgamate with the horseshoe vortex, but a continually larger portion of the far-field vorticity packets pass directly into the gap. As the amount of vorticity lost to the gap increases, the horseshoe vortex weakens even more quickly, and is entrained and swept into the gap much earlier in a cycle.

As the gap clearance is even further increased (4.4%D), eventually all of the far-field vorticity packets are carried directly into the gap, bypassing amalgamation with the horseshoe vortex. Even further increases in the gap clearance (5.4%D) result in a portion of the near-field vorticity packets passing into the freestream, bypassing the horseshoe vortex, and entering the gap.

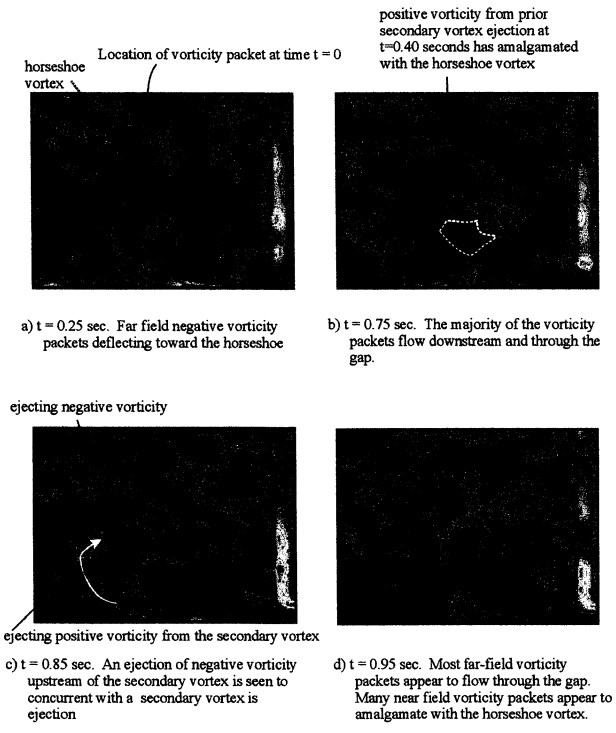

Figure 7 : Vorticity distributions for 3.0% gap

The transport behavior of vorticity packets can be inferred from the illustration shown in figure 8. For no clearance gap and a 1.7%D gap clearance, a far-field vorticity packet, indicated by the round marker, follows a streamline back to the horseshoe vortex. For the larger gap clearances, it is likely that a vorticity packet originating in this same location would be swept into the gap (e.g. figure 8c,d). The path of a near-field vorticity packet, originating at a location indicated by the triangular marker, will interact directly with the horseshoe vortex until the clearance gaps becomes large---somewhere between 3.3%D and 4.0%D, as suggested by figure 8d.

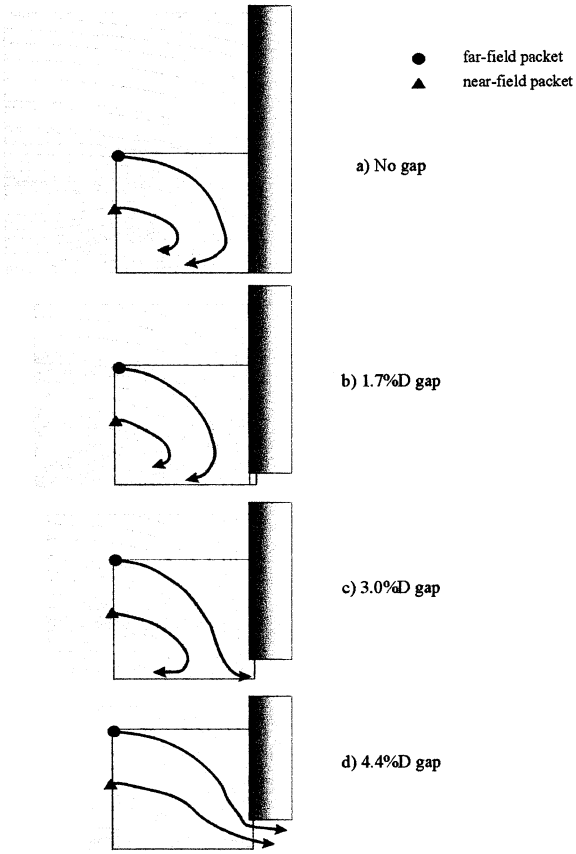

Figure 8: Schematic of path of near-field and far-field vorticity packets

CONCLUSIONS

Based on the present study, it is concluded that the continued presence and behavior of the turbulent juncture horseshoe vortex system is greatly dependent on its amalgamation with both the far and near-field vorticity packets. These far-field packets are generated upstream of the juncture, apparently due to the normal turbulence production process, and upon encountering the bluff body, recirculate back to reinforce the dominant horseshoe vortex. Near-field vorticity packets are generated during ejection of secondary vortices due to viscous interaction of the horseshoe vortex with the end wall surface. These latter structures almost immediately amalgamate with the horseshoe vortex. It is this sporadic, but

continued, interaction with boundary layer vortex packets that sustains the strength of the turbulent horseshoe vortex system, and precipitates the unsteady behavior of the system. The presence of a clearance gap provides a conduit for these impinging vorticity packets to escape the juncture region, which can consequently result in a less stable, weaker horseshoe vortex system, particularly as the

clearance gap is increased. When a clearance gap grows beyond roughly 5% of the body diameter, the loss of the vorticity in vorticity packets can result in the complete breakdown and elimination of the horseshoe vortex system.

REFERENCES

Acalar, M.S. and Smith, C.R., 1987, "A Study of Hairpin Vortices in a Laminar Boundary Layer," *Journal of Fluid Mechanics*, Vol. 175, pp. 1-41.

Adrain, R.J., 1991, "Particle-Imaging Techniques for Experimental Fluid Mechanics." *Annual Review of Fluid Mechanics*, Vol. 23, pp. 261-304.

Adrian, R.J., Meinhart, C.D., and Tomkins, C.D., 1999, "Vortex Organization in the Outer Region of the Turbulent Boundary Layer", University of Illinois at Urbana-Champaign, TAM Report No. 924.

Marini, B.D., 2000, "A Combined Flow-Field/Temperature-Field Study of the Impact of Blade Tip Clearance on Turbomachinery–Type Blading", Ph.D. Dissertation, Lehigh University.

Praisner, T.J., 1998, "Investigation of Turbulent Juncture Flow Heat Transfer", Ph.D. dissertation, Lehigh University.

Rockwell, D.R., Magness, C., Towfighi, J., Akin, O. and Corcoran, T., 1993, "High Image-Density Particle Image Velocimetry Using Laser Scanning Techniques", *Experiments in Flu*ids, Vol. 14, pp. 181-192.

Sabatino, D.R., 2000, "Boundary Layer, Grid Turbulence, and Periodic Wake Effects on Turbulent Juncture Flows" Ph.D. dissertation, Lehigh University.